Orientation Dependence of the Intrinsic Anomalous Hall Effect in hcp Cobalt

Eric Roman, Yuriy Mokrousov, and Ivo Souza
Department of Physics, University of California, Berkeley, California 94720, USA
(Received 1 May 2009; published 27 August 2009)

We carry out first-principles calculations of the dependence of the intrinsic anomalous Hall conductivity of hcp Co on the spin magnetization direction. The Hall conductivity drops from 481 to 116 S/cm as the magnetization is tilted from the easy axis (c axis) to the ab plane. These values agree reasonably well with measurements on single crystals, while the angular average of 226 S/cm is in excellent agreement with the value of 205 S/cm measured in polycrystalline films. The strong intrinsic anisotropy is shown to arise from quasidegeneracies near the Fermi level.

DOI: 10.1103/PhysRevLett.103.097203 PACS numbers: 75.30.Gw, 72.15.Gd, 78.20.Ls

The Hall effect in ferromagnets has two parts: an ordinary Lorentz-force part proportional to the magnetic field and an "anomalous" part which instead depends on the magnetization. In collinear ferromagnets the anomalous Hall effect (AHE) results from the interplay between spin polarization (exchange splitting) and spin-orbit interaction, and has several contributions. Karplus and Luttinger (KL) [1] showed that, as a consequence of virtual interband transitions, electrons moving in the spin-orbit-coupled bands acquire an *anomalous velocity* transverse to the electric field whose sum over all occupied bands is nonzero in ferromagnets. Another contribution comes from the spin-orbit-induced asymmetry in the impurity scattering of the spin-polarized charge carriers; the anomalous Hall resistivity $\rho^a_{yx} = E_y/J_x$ arising from this skew-scattering process scales linearly with the longitudinal resistivity ρ_{xx}. An additional scattering process, side jump (SJ), yields a quadratic scaling, the same as for the KL contribution. For a review, see Ref. [2].

The development of a predictive theory of the AHE has been hampered by the difficulty in evaluating the scattering (extrinsic) contributions for real materials. On the other hand, progress was made recently in calculating the intrinsic contribution [3–6]. The KL anomalous Hall conductivity (AHC) $\sigma^a_{ij} = -\sigma^a_{ji}$ depends only on the band structure of the perfect crystal, and is given by

$$\boldsymbol{\sigma}^a = -\frac{e^2}{\hbar}\int_{\mathrm{BZ}}\frac{d^3k}{(2\pi)^3}\boldsymbol{\Omega}_{\mathbf{k}}. \tag{1}$$

Here $\boldsymbol{\sigma}^a$ is the AHC vector, with components $\sigma^a_k = (1/2)\epsilon_{ijk}\sigma^a_{ij}$, and $\boldsymbol{\Omega}_{\mathbf{k}} = \sum_n f_{n\mathbf{k}}\boldsymbol{\Omega}_{n\mathbf{k}}$, where $f_{n\mathbf{k}}$ is the Fermi-Dirac distribution and $\boldsymbol{\Omega}_{n\mathbf{k}}$ is the Berry curvature vector of each Bloch state. First-principles calculations for Fe, Co, Ni [4–6], $SrRuO_3$ [3], and Mn_5Ge_3 [7] have consistently found agreement in sign and magnitude—often to within better than 30%—with room-temperature experiments, establishing the importance of the KL contribution in moderately conducting samples of itinerant ferromagnets (skew scattering tends to dominate in high-purity samples at low temperatures).

One of the key experimental challenges is to isolate the various contributions to the AHE. Often, skew scattering can be separated from the other two terms by fitting the anomalous Hall resistivity to the form

$$\rho^a_{yx} = a\rho_{xx} + b\rho^2_{xx}, \tag{2}$$

where $b = \sigma^a_{xy} + b^{\mathrm{SJ}}$. The coefficients a (skew scattering) and b (intrinsic plus side jump) can be read off a plot of ρ^a_{yx}/ρ_{xx} versus ρ_{xx}, where ρ_{xx} is varied through doping or temperature changes. This analysis does not distinguish between the KL and SJ contributions, and efforts to separate them are ongoing [2,8]. At present it is common practice to rely on first-principles calculations for that purpose: when reasonable agreement is found between Eq. (1) and the measured coefficient b, it is taken as an indication that the KL contribution dominates. That conclusion is strengthened if the calculations are able to account for the observed dependence on some well-controlled parameter, such as the temperature-dependent magnetization [3,7]. Searching for additional experimental signatures of the intrinsic AHE is therefore an important goal for *ab initio* theory.

In this Letter, we show that the AHC of hcp Co single crystals displays a strong dependence on the magnetization direction relative to the crystal axes, in agreement with the pioneering experiment of Volkenshtein *et al.* [9] (anisotropy in the AHE has also been observed in hcp Gd, fcc Ni, and bcc Fe, as well as several magnetic compounds [10,11]). The theoretical description of anisotropy has so far been mostly phenomenological; to our knowledge, the only attempt at a microscopic model has been the tight-binding study of Ref. [11]. Because the AHC is sensitive to fine details in the band structure [3–6], a quantitative *ab initio* study is highly desirable. It is also not obvious that the phenomenological description of magnetocrystalline anisotropy [12] applies to the AHC given by Eq. (1). The total Berry curvature $\boldsymbol{\Omega}_{\mathbf{k}}$ of the occupied states undergoes strong and rapid variations in k space, with sharp

peaks and valleys from avoided crossings near the Fermi level [3–5]. It has been argued that such features cannot be described perturbatively [4], and there is numerical evidence that they give rise to a complex or even irregular behavior of the AHC as a function of exchange splitting and Fermi level position [3]. This raises the possibility that the orientation dependence of $\boldsymbol{\sigma}^a$ may also not be smooth. We find instead that in hcp Co it is remarkably smooth, and can be described by a phenomenological expression.

We begin by reviewing the phenomenology [12]. Electrical conduction in ferromagnets is described by a magnetization-dependent conductivity tensor: $J_i = \sigma_{ij}(\mathbf{M}_s)\mathcal{E}_j$, with i, j Cartesian indices. The Onsager relation implies that the symmetric (σ^s_{ij}) and antisymmetric (σ^a_{ij}) parts of σ_{ij} are, respectively, even and odd functions of the (spin) magnetization $\mathbf{M}_s$. The current density $\mathbf{J}$ is therefore comprised of an even (Ohmic) part $\mathbf{J}^s = \boldsymbol{\sigma}^s \cdot \boldsymbol{\mathcal{E}}$, and an odd (Hall) part $\mathbf{J}^a = \boldsymbol{\mathcal{E}} \times \boldsymbol{\sigma}^a$. Note that $\mathbf{J}^a$ is perpendicular to the electric field $\boldsymbol{\mathcal{E}}$ but not necessarily to $\mathbf{M}_s$, as $\boldsymbol{\sigma}^a$ and $\mathbf{M}_s$ may not be parallel. Such noncollinearity is the signature of the anisotropic AHE.

It seems plausible that the actual degree of anisotropy will vary significantly among the various mechanisms [13]. Standard treatments of skew scattering lead to an isotropic Hall current $\mathbf{J}^a \perp \mathbf{M}_s$ [14,15], but the inclusion of band structure effects [16] may introduce anisotropy. The intrinsic AHE, on the other hand, is purely a band structure effect, and thus inherently anisotropic. It was noted by Fivaz [15] that its anisotropy can be resonantly enhanced by quasidegeneracies near the Fermi level, a feature which is borne out by our calculations.

To characterize the anisotropy we express the AHC vector $\boldsymbol{\sigma}^a$ in a Cartesian frame aligned with $\mathbf{M}_s = M\hat{\mathbf{m}}_s$:

$$\boldsymbol{\sigma}^a = \sigma_m \hat{\mathbf{m}}_s + \sigma_\theta \hat{\boldsymbol{\theta}} + \sigma_\varphi \hat{\boldsymbol{\varphi}}, \tag{3}$$

where θ and φ are, respectively, the polar and azimuthal angles of $\mathbf{M}_s$ relative to the c and a axis. In systems with a net magnetization but otherwise macroscopically isotropic (e.g., ferromagnetic polycrystals) $\boldsymbol{\sigma}^a \parallel \hat{\mathbf{m}}_s$, while in single crystals that is only guaranteed for $\mathbf{M}_s$ pointing along certain high-symmetry directions. The orientation dependence in hcp crystals is given to third order in a spherical-harmonic expansion by [17]

$$\begin{aligned} \sigma^a_1 &= c_{11}\bar{Y}_{11} + c_{31}\bar{Y}_{31} \\ \sigma^a_2 &= c_{11}\bar{Y}_{1,-1} + c_{31}\bar{Y}_{3,-1} \\ \sigma^a_3 &= c_{10}\bar{Y}_{10} + c_{30}\bar{Y}_{30}, \end{aligned} \tag{4}$$

where $\bar{Y}_{lm}(\theta, \varphi)$ are real spherical harmonics, and σ^a_1 and σ^a_3 point along the a and c axis. Since σ^a_3 is independent of φ while σ^a_1 and σ^a_2 have, respectively, cosine and sine dependencies, $\boldsymbol{\sigma}^a$ and $\mathbf{M}_s$ share the same azimuthal angle, and their polar-angle mismatch is independent of φ. Thus in Eq. (3) $\sigma_{m,\theta} = \sigma_{m,\theta}(\theta)$ and $\sigma_\varphi = 0$.

Using the methods described in Ref. [17], the AHC of hcp Co was calculated for several orientations of the magnetization in the ac plane ($\varphi = 0$). The tilting angle θ was increased from 0 ($\mathbf{M}_s \parallel c$ axis) to $\pi/2$ ($\mathbf{M}_s \parallel a$ axis) in steps of $\pi/32$, and for each step the vector $\boldsymbol{\sigma}^a(\theta, \varphi)$ was calculated. Figure 1 contains the numerical results: $\sigma_m(\theta, 0)$ and $\sigma_m(\theta, 0)$ are shown in the main panels, while the insets contain additional data which confirm the absence of (or very weak) basal-plane anisotropy. The vectors $\boldsymbol{\sigma}^a$ and $\mathbf{M}_s$ start out parallel, but as $\mathbf{M}_s$ tilts away from the c axis $\boldsymbol{\sigma}^a$ lags behind ($\sigma_\theta < 0$), and they become parallel again upon reaching the ab plane. The angular dependence is smooth, and can be described by Eq. (4). A least-squares fitting to the data yields, in S/cm, $c_{10} = 951.5$, $c_{11} = -204.1$, $c_{30} = 1.2$, and $c_{31} = 38.4$, producing the solid-line curves in Fig. 1.

The calculated AHC is strongly anisotropic, decreasing by a factor of 4.1 between $\theta = 0$ and $\theta = \pi/2$. In Ref. [9] a ratio of 2.93 was found between the c axis and ab plane Hall resistivities of single crystals at 290 K. This translates into an AHC ratio of $(\rho_{zz}/\rho_{xx})2.93 = 5.43$, close to our calculated value (the prefactor $\rho_{zz}/\rho_{xx} = 1.854$ accounts for the anisotropy in the Ohmic resistivity [17]).

We now turn to the comparison with the measurements on polycrystalline films magnetized along the growth direction [18]. At saturation the absolute magnetization direction is the same in every crystallite, while its orientation relative to the crystal axes varies from one crystallite to another. It is difficult to calculate rigorously the effective conductivity of a composite medium, and we shall estimate the effective AHC by stipulating that (i) the crystallites are randomly oriented, (ii) each possesses a bulklike Hall conductivity $\boldsymbol{\sigma}^a(\theta, \varphi)$ which depends only on its orientation, and (iii) every crystallite feels the same electric field $\boldsymbol{\mathcal{E}}$. The net Hall current density in the films is then given by the orientational average $\langle \mathbf{J}^a \rangle = \boldsymbol{\mathcal{E}} \times \langle \boldsymbol{\sigma}^a \rangle$. It is clear from

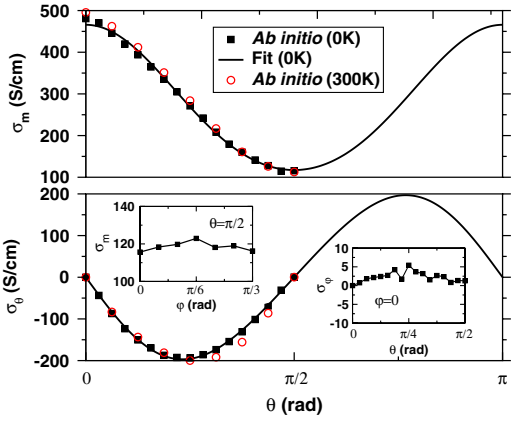

FIG. 1 (color online). Evolution of the components of the anomalous Hall conductivity parallel (σ_m) and perpendicular (σ_θ) to the spin magnetization [Eq. (3)] as $\mathbf{M}_s$ is tilted by θ from the c axis towards the a axis. The solid lines are fits to the first-principles data, as described in the text. The left and right insets show, respectively, $\sigma_m(\pi/2, \varphi)$ and $\sigma_\varphi(\theta, 0)$.

Fig. 1 and Eq. (3) that $\langle \boldsymbol{\sigma}^a \rangle$ points along $\mathbf{M}_s$; its value is $\sigma^a_{\rm av} = \int_0^{\pi/2} \sigma_m(\theta) \sin\theta d\theta = 226$ S/cm, close to the value $b = 205$ S/cm obtained in Ref. [18] by fitting the Hall resistivity to Eq. (2). The close agreement reinforces the conclusion [18] that the KL contribution to b dominates over SJ.

Table I summarizes the comparison of the calculated intrinsic AHC with experiments. For polycrystals the agreement is excellent, while in the case of single crystals the sign and magnitude of the anisotropy are correct, but the calculated AHC values are somewhat smaller than the experimental ones, especially along the c axis. In making such comparisons the limitations of both theory (e.g., the use of an approximate density functional) and experiment should be kept in mind [6]. We note, in particular, that while in Ref. [18] both the Hall and Ohmic resistivities were measured over a range of temperatures in order to isolate the intrinsic contribution, Ref. [9] only reports the room-temperature Hall resistivities, making the comparison with our calculations more difficult.

Next we discuss the origin of the strong anisotropy. The AHC of uniaxial crystals is anisotropic to first order in the magnetization [17], while in cubic crystals anisotropy appears only in third order, and is expected to be much weaker. For example, the calculated AHC of fcc Co changes by less than 10% as a function of orientation (Table I). Perhaps more surprising is the fact that in hcp Co the AHE appears to be considerably more anisotropic than both the magneto-optical spectrum [19] and the orbital magnetization [20]. This is intriguing because the three phenomena are related by sum rules [21], and hence anisotropy appears at the same order.

The sum rules read $\langle \omega^{-1} \mathrm{Im}\boldsymbol{\sigma}^a \rangle_\omega = (\pi/2)\boldsymbol{\sigma}^a(\omega = 0)$ and $\langle \mathrm{Im}\boldsymbol{\sigma}^a \rangle_\omega = (\pi e c/\hbar)\mathbf{M}^{(\mathrm{I})}_{\rm SR}$, where $\langle f \rangle_\omega = \int_0^\infty f(\omega) d\omega$. $\boldsymbol{\sigma}^a(\omega = 0)$ is the dc AHC; at finite frequencies $\boldsymbol{\sigma}^a$ acquires an imaginary part which describes the magnetic circular dichroism (MCD). The first sum rule expresses the intrinsic AHC in terms of the first inverse moment of the interband MCD spectrum. The second relates $\mathbf{M}^{(\mathrm{I})}_{\rm SR}$, the "gauge-invariant self-rotation" part of $\mathbf{M}_{\rm orb}$, to the zeroth spectral moment [21]. The absorptive part of $\sigma_m(\omega)$ was calculated [17] and is plotted in the upper panel of Fig. 2 for $\theta = 0, \pi/2$. The lower panel shows the AHC sum rule frequency integral as a function of the lower limit of integration. While for either orientation there are sizable contributions to the AHC up to $\omega \sim 3.5$ eV, the orientation dependence is concentrated below 0.3 eV. At these low frequencies the MCD spectrum changes sign between $\theta = 0$ and $\theta = \pi/2$. This difference gets magnified in the AHC via the inverse-frequency weight factor, producing the bifurcation of the two curves in the lower panel. All frequencies are equally weighted in the orbital moment sum rule, which as a result is more isotropic, as seen in the inset.

TABLE I. Anomalous Hall conductivity in S/cm for selected high-symmetry orientations of the magnetization in hcp and fcc Co. The polycrystalline AHC is calculated as an orientational average (see text), and the Hall resistivities of Ref. [9] were converted into conductivities as detailed in Ref. [17].

Co	Orientation	Calculated	Experiment
hcp	c axis	481	~813[a]
	ab plane	116	~150[a]
	Polycrystal	226	205[b]
fcc	[001]	249	
	[110]	218	
	[111]	234	

[a]Reference [9]
[b]Reference [18]

It is clear from the above that the anisotropy of the intrinsic AHC is dominated by low-frequency interband transitions. Such transitions couple quasidegenerate states on opposite sides of the Fermi level, and to see their role more directly we turn to Fig. 3. The upper panel displays the energy bands near E_F. Rotating $\mathbf{M}_s$ from the c axis to the a axis in the presence of the spin-orbit interaction turns various band crossings into avoided crossings and vice versa. When this occurs close to the Fermi level, $-\boldsymbol{\Omega}_{\mathbf{k}} \cdot \hat{\mathbf{m}}_s$ can flip sign in the process while retaining the large magnitude which is typical of (anti)crossings at E_F [3–5]. This is what happens near the zone-boundary point L, as seen in the middle and lower panels.

How can the spiky behavior of $\boldsymbol{\Omega}_{\mathbf{k}}$ be reconciled with the smooth angular dependence of $\boldsymbol{\sigma}^a$? According to the phenomenological expression (4), $\sigma^a_i \propto M_i$ $(i = x, y, z)$ to leading order in $\mathbf{M}_s$. That will be the case for the intrinsic AHC provided that in Eq. (1) $\Omega_{\mathbf{k},i} \propto M_i$ at each $\mathbf{k}$. This proportionality holds reasonably well even around strong

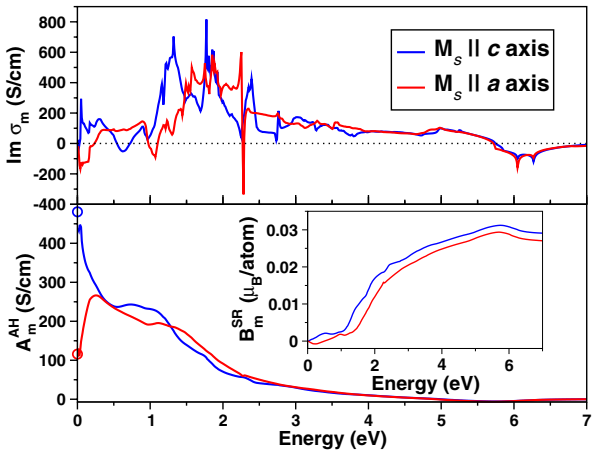

FIG. 2 (color online). Upper panel: Interband MCD spectrum for two magnetization directions. Lower panel: Cumulative contribution to the AHC from the spectrum above energy $\hbar\omega$, $A^{\rm AH}_m(\omega) = \frac{2}{\pi}\int_\omega^{\omega_{\max}} \frac{1}{\omega'} \mathrm{Im}\sigma_m(\omega') d\omega'$, truncated at $\omega_{\max} = 7$ eV. Circles denote the AHC calculated directly from Eq. (1). Inset: Cumulative contribution to the gauge-invariant self-rotation per atom from the spectrum below energy $\hbar\omega$, $B^{\rm SR}_m(\omega) = \frac{V_c \hbar}{2\pi e c}\int_0^\omega \mathrm{Im}\sigma^a_m(\omega') d\omega'$ (V_c is the cell volume).

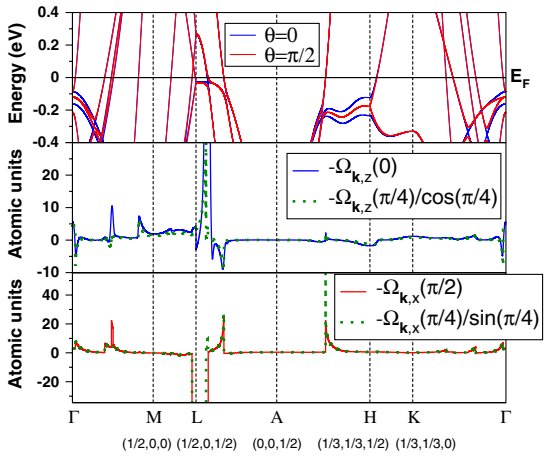

FIG. 3 (color online). Upper panel: Energy bands close to the Fermi level for $\mathbf{M}_s \parallel c$ axis ($\theta = 0$) and $\mathbf{M}_s \parallel a$ axis ($\theta = \pi/2$). Middle and lower panels: Berry curvature $\mathbf{\Omega}_\mathbf{k}$ for $\theta = 0$, $\theta = \pi/2$, and $\theta = \pi/4$. The full height of the resonance peaks near the L point is of the order of 10^3 a.u. The high-symmetry points are given in lattice coordinates.

resonance peaks, judging from the comparison in Fig. 3 between $\mathbf{\Omega}_\mathbf{k}$ for $\theta = \pi/4$ and for $\theta = 0, \pi/2$.

We end with a discussion of temperature effects. The calculated AHC hardly changes as the Fermi-smearing temperature in Eq. (1) is varied from 0 to 300 K (Fig. 1). This agrees with the constancy of the coefficient b from 78 to 350 K [18]. Thermal fluctuations in $\hat{\mathbf{m}}_s$ can also give rise to a T dependence of the AHC: if at $T = 0$ σ_i^a changes linearly with M_i upon rotating $\mathbf{M}_s$ then $\boldsymbol{\sigma}^a(T) = [M(T)/M(0)]\boldsymbol{\sigma}^a(0)$, a behavior seen in Mn_5Ge_3 [7]. Figure 4 shows that in hcp Co σ_z^a depends linearly on M_z, while the $\sigma_x^a(M_x)$ curve is significantly nonlinear. As a result, the a-axis AHC should decrease with T faster than $M(T)$, producing an increase in the ratio $\sigma_z^a(\theta = 0)/\sigma_x^a(\theta = \pi/2)$. A quantitative estimate can be made (see Ref. [17] for details). The result, shown in the inset

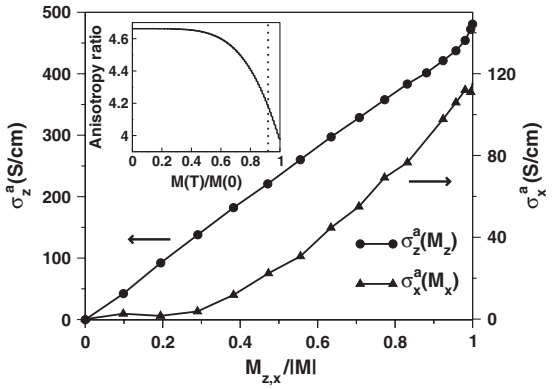

FIG. 4. Evolution of $\boldsymbol{\sigma}^a$ as the magnetization is rotated in the ac plane, plotted as $\sigma_z^a(\cos\theta)$ and $\sigma_x^a(\sin\theta)$. Inset: Anisotropy ratio $\sigma_z^a(\theta = 0)/\sigma_x^a(\theta = \pi/2)$ versus the reduced magnetization, according to the spin-fluctuation model [17]. The dotted line denotes the approximate location of the hcp → fcc transition.

of Fig. 4, is a 17% increase between 0 K and T_c. This effect is, however, preempted by the phase transformation into the fcc structure at 695 K.

In summary, we have shown that the intrinsic AHC of single crystals of hcp Co depends strongly on the magnetization direction, decreasing by a factor of 4 between the c axis and ab plane orientations. The calculated AHCs agree in sign and compare fairly well in magnitude with single-crystal measurements, and averaging over orientations yields close agreement with measurements on polycrystalline films. The anisotropy of the AHE provides a stringent test for quantitative theories, and our findings support the emerging viewpoint that the AHE of transition metal ferromagnets is largely intrinsic.

The authors wish to thank David Vanderbilt, Jonathan Yates, and Xinjie Wang for fruitful discussions. This work was supported by NSF Grant No. DMR 0706493. Y. M. was supported by DFG project MO 1731/1-1. Computational resources have been provided by NERSC.

[1] R. Karplus and J. M. Luttinger, Phys. Rev. **95**, 1154 (1954).
[2] N. Nagaosa *et al.*, arXiv:0904.4154.
[3] Z. Fang *et al.*, Science **302**, 92 (2003).
[4] Y. Yao *et al.*, Phys. Rev. Lett. **92**, 037204 (2004).
[5] X. Wang *et al.*, Phys. Rev. B **74**, 195118 (2006).
[6] X. Wang *et al.*, Phys. Rev. B **76**, 195109 (2007).
[7] C. Zeng *et al.*, Phys. Rev. Lett. **96**, 037204 (2006).
[8] Y. Tian, L. Ye, and X. Jin, Phys. Rev. Lett. **103**, 087206 (2009).
[9] N. V. Volkenshtein, G. V. Fedorov, and V. P. Shirokovskii, Phys. Met. Metallogr. **11**, 151 (1961).
[10] R. S. Lee and S. Legvold, Phys. Rev. **162**, 431 (1967); T. Hiraoka, J. Sci. Hiroshima Univ., Ser. A-II **32**, 153 (1968); A. A. Hirsch and Y. Weissman, Phys. Lett. A **44**, 239 (1973); B. C. Sales, R. Jin, and D. Mandrus, Phys. Rev. B **77**, 024409 (2008); J. Stankiewicz and K. P. Skokov, Phys. Rev. B **78**, 214435 (2008).
[11] K. Ohgushi, S. Miyasaka, and Y. Tokura, J. Phys. Soc. Jpn. **75**, 013710 (2006).
[12] R. R. Birss, *Symmetry and Magnetism* (North-Holland, Amsterdam, 1964).
[13] In particular, the KL and SJ contributions, which have the same dependence on ρ_{xx}, tend to have quite difference dependencies on more specific system parameters [2].
[14] F. E. Maranzana, Phys. Rev. **160**, 421 (1967).
[15] R. C. Fivaz, Phys. Rev. **183**, 586 (1969).
[16] P. Leroux-Hugon and A. Ghazali, J. Phys. C **5**, 1072 (1972).
[17] See EPAPS Document No. E-PRLTAO-103-036937 for supplementary material. For more information on EPAPS, see http://www.aip.org/pubservs/epaps.html.
[18] J. Kötzler and W. Gil, Phys. Rev. B **72**, 060412(R) (2005).
[19] D. Weller *et al.*, Phys. Rev. Lett. **72**, 2097 (1994).
[20] D. Ceresoli *et al.*, arXiv:0904.1988.
[21] I. Souza and D. Vanderbilt, Phys. Rev. B **77**, 054438 (2008).